Identification of Enzyme−Substrate and Enzyme−Product Complexes in the Catalytic Mechanism of Glucoamylase from *Aspergillus awamori*

Sateesh K. Natarajan[§] and Michael R. Sierks*

Department of Chemical and Biochemical Engineering, University of Maryland Baltimore County, Baltimore, Maryland 21228

Received June 7, 1996; Revised Manuscript Received August 12, 1996[⊗]

ABSTRACT: Intermediates in the catalytic mechanism of *Aspergillus awamori* glucoamylase (GA) were identified by studying pre-steady-state and steady-state kinetics of the wild-type GA/maltose and Trp120 → Phe GA/maltotriose reactions in H_2O and D_2O. Pre-steady-state fluorescence signal analysis was carried out to ascertain the relative intrinsic fluorescence of the enzyme intermediates. A three-step minimal pathway for oligosaccharide hydrolysis represented by $E + G_x$ (k_1) ⇄ (k_{-1}) EG_x (k_2) ⇄ (k_{-2}) EP (k_{cat}) → $E + P$ is proposed. The first step, represented by the association constant K_1 (k_1/k_{-1}), depicts the fast formation of enzyme−substrate complex and is the primary factor in fluorescence quenching. A 2.7-fold increase in K_1 with D_2O as solvent is observed with both enzymes due to the cumulative effect of deuterium on complex hydrogen bonding at the active site. The second step further quenches the enzyme fluorescence and is identified as the hydrolytic step, forming an enzyme−product complex. Both k_2 and k_{-2} values show similar 2-fold decreases in D_2O for both enzymes, consistent with the microscopic reversibility of the hydrolytic reaction. The solvent isotopic effect on the hydrolytic step is likely due to either abstraction of an exchangeable proton from the general acid Glu179 or directed addition of water to the oxocarbonium ion intermediate by the general base Glu400. No significant isotope effect was observed on the steady-state k_{cat} value for wild-type GA with maltose, indicating a nonhydrolytic step as rate-limiting. The third step, a posthydrolytic rate-determining step, is the product release as evident from steady-state kinetics with wild-type and Trp120 → Phe GAs using α-D-glucosyl fluoride.

Glucoamylase (GA)[1] (1,4-α-D-glucan glucohydrolase, E.C. 3.2.1.3) is an exohydrolase which hydrolyzes D-glucose from the nonreducing ends of starch and related poly- and oligosaccharides. GA hydrolyzes both α-1,4 and α-1,6 glucosidic linkages at a single active site (Hiromi et al., 1966a), although the α-1,4 linkages are cleaved much more efficiently. The catalytic mechanism of GA is fairly flexible, as α-D-glucosyl fluoride (GF) (Kitahata et al., 1981) and *p*-nitrophenyl α-D-glucoside (Selwood & Sinnott, 1990) can also be hydrolyzed to glucose. Two catalytic carboxyl groups have been identified in the GA hydrolytic mechanism (Hiromi et al., 1966b), Glu179 of *Aspergillus awamori* GA as the general catalytic acid residue (Sierks et al., 1990) and Glu400 as the catalytic base (Harris et al., 1993; Frandsen et al., 1994). Hydrolysis is postulated to be initiated by proton donation from Glu179 to the scissile glycosidic oxygen of the substrate, followed by Glu400-guided nucleophilic addition of water to the oxocarbonium ion at the C-1 carbon of the aglycon moiety (Frandsen et al., 1994).

The GA active site consists of seven subsites capable of accommodating glucosyl residues with the catalytic carboxylic groups located between subsites 1 and 2 (Hiromi et al., 1966a,b, 1983). In the subsite theory postulated to account for the action pattern of amylases, the hydrolytic step is assumed to be the rate-limiting step of the reaction. This assumption was based on pre-steady-state kinetic studies on the hydrolysis of *o*-nitrophenyl α-maltoside by *Bacillus subtilis* α-amylase (Suetsugu et al., 1971), where the lack of a nitrophenol burst was concluded to indicate hydrolysis as the slowest step in the reaction. The lack of a nitrophenol burst, however, merely indicates the products are released at similar rates. Such a hydrolysis-limited catalytic mechanism was assumed to account for most amylases including glucoamylase (Hiromi, 1972) in the absence of any evidence to the contrary. However, several studies have demonstrated that the assumption that hydrolysis is the rate-limiting step of GA is questionable. The turnover rates of *Rhizopus delemar* GA with maltooligosaccharides are significantly lower than the rates of the comparable *Rhizopus niveus* GA with α-D-glucosyl fluoride, giving the first indication that the release of part of the maltooligosaccharide substrate unproductively bound after hydrolysis may be a very slow step (Kitahata et al., 1981). Additional evidence has also been obtained by studying the differences in kinetic behavior of wild-type, Asp176 → Asn, Glu400 → Gln, and Trp120 loop mutant GAs of *A. awamori* toward GF and oligosaccharides which strongly suggest that the release of the reducing-end sugars is the rate-limiting step of the catalytic mechanism for oligosaccharide hydrolysis (Sierks & Svensson, 1996; Natarajan & Sierks, 1996).

Pre-steady-state kinetic analysis of glucoamylases from *R. niveus* (Tanaka et al., 1982) and *Aspergillus niger* (Olsen et al., 1992, 1993) with maltodextrin substrates have suggested a three-step reaction pathway (eq 1) involving a fast but weak bimolecular enzyme−ligand association, followed by a unimolecular rearrangement resulting in a tight enzyme−substrate complex, followed by hydrolysis to yield products and the free enzyme. The breakdown of the enzyme−

* Corresponding author.

§ Present address: Department of Pathology, Johns Hopkins Medical Institutions, Baltimore, MD 21205.

⊗ Abstract published in *Advance ACS Abstracts,* November 1, 1996.

[1] Abbreviations: GA, glucoamylase; GF, α-D-glucosyl fluoride.

S0006-2960(96)01355-4 CCC: $12.00

substrate intermediate EG_x*, i.e., the enzyme complex preceding the transition state of the hydrolytic step, was postulated to be rate-limiting.

$$E + G_x \underset{k_{-1}}{\overset{k_1}{\rightleftharpoons}} EG_x \underset{k_{-2}}{\overset{k_2}{\rightleftharpoons}} EG_x^* \xrightarrow{k_3} E + P \qquad (1)$$

The observed fluorescence intensity decrease associated with *R. niveus* GA interactions with maltose was shown to occur solely during the slow unimolecular step (Tanaka et al., 1982) and this was assumed to also hold with *A. niger* GA (Olsen et al., 1992, 1993), although without experimental evidence. In this work, we have carried out a rigorous analysis of the fluorescence quenching observed in reactions with *A. awamori* GA, which is identical to *A. niger* GA, to quantitatively determine the magnitude of fluorescence quenched in each step of the enzyme mechanism. We have used the resulting information about the magnitude of fluorescence quenched in each step to gain insight about the nature of the individual steps.

Comparison of enzyme rate measurements in H_2O and D_2O has long been a useful tool in mechanistic investigations, particularly for the study of proton transfer steps. Here we have determined the pre-steady-state and steady-state kinetic rate parameters in H_2O and D_2O to identify the bond hydrolytic step, which involves proton transfers, in the *A. awamori* GA mechanism. Since, for oligosaccharide hydrolysis by GA, product release has been suggested as the rate-limiting step (Sierks & Svensson, 1996; Natarajan & Sierks, 1996) and since there may only be three distinguishable steps in the catalytic mechanism (Olsen et al., 1993), it seemed reasonable to postulate that the second step in the GA mechanism depicted in eq 1 was actually the chemical hydrolytic step rather than the suggested prehydrolytic unimolecular readjustment step. The glucosidic bond hydrolysis rate by GA is expected to decrease in D_2O. We determined the pre-steady-state kinetic parameters for the wild-type GA reaction in H_2O and D_2O buffers to test if the unimolecular rearrangement is the hydrolytic step. Trp120, which has a crucial role in product release, is not directly involved in the chemistry of the bond hydrolysis, as evident from kinetic behavior of Trp120 → Phe GA toward maltose and GF (Natarajan & Sierks, 1996). Therefore, any solvent isotope effects are expected to alter the chemistry of bond hydrolysis for both Trp120 → Phe and wild-type GA reactions similarly. So, pre-steady-state kinetic parameters of Trp120 → Phe GA reaction in H_2O and D_2O buffers were also determined to further investigate the chemical nature of the unimolecular step. A significant isotope effect is expected on the steady-state turnover rate of an enzyme whose reaction pathway consists of one or more proton transfers, providing the proton transfer step is rate-limiting. The bond hydrolytic step was concluded to be rate-determining for *p*-nitrophenyl glucoside hydrolysis by *A. niger* GA based on a nearly 2-fold decrease of k_{cat} in D_2O (Selwood & Sinnott, 1990). Here, the steady-state kinetic parameters were obtained in H_2O and D_2O buffers for maltose hydrolysis by wild-type GA to determine if the hydrolytic step is rate-constricting for oligosaccharide substrates.

Pre-steady-state kinetic data provide little or no information about the rate-limiting step of reactions, while steady-state catalytic turnovers are often a measure of the the slowest step. Therefore, the pre-steady-state and steady-state kinetic results need to be linked to obtain a more complete picture of the reaction. Release of the reducing-end sugars after hydrolysis is likely the slowest step in the *A. awamori* GA mechanism as indicated by k_{cat}/K_m values determined with wild-type and mutant GAs with GF and maltose (Sierks & Svensson, 1996; Natarajan & Sierks, 1996). Limited substrate availability did not permit calculation of the individual k_{cat} and K_m with GF in those studies. In the present work, individual k_{cat} and K_m values of wild-type and Trp120 → Phe GA were determined with GF at 8 °C to provide further insight into the argument that release of bound products is the rate-limiting step of oligosaccharide hydrolysis. The results of pre-steady-state and steady-state kinetic studies are consolidated to present a more complete picture of the GA enzyme mechanism for oligosaccharide hydrolysis.

MATERIALS AND METHODS

Materials. Wild-type and Trp120 → Phe GA genes (Sierks et al., 1989) were expressed in *Saccharomyces cerevisiae* and purified essentially as described (Natarajan & Sierks, 1996). Maltose, maltotriose, α-glucosyl fluoride (GF), glucose oxidase kit for glucose determination, D_2O (99.9 atom % D) and acetic acid-*d* (CH_3COOD, 98 atom % D) were purchased from Sigma (St. Louis, MO).

Buffers. For all the studies, a 0.05 M sodium acetate buffer of pH 4.5 in H_2O and pD 5.0 in D_2O was used. The pK_as of most common weak acids including acetic acid are higher in D_2O compared to H_2O by about 0.5 unit (Quinn & Sutton, 1991). Assuming no gross structural deformations on deuteration, the optimum pD of enzymes usually increases by an amount approximately equal to the shift in the pK_a of the acid component of the buffer in D_2O (Schowen, 1976). Therefore the pD of the D_2O buffer used was 0.5 unit higher than the pH of the H_2O buffer. Also, the pK governing k_{cat} for *p*-nitrophenyl α-D-glucoside hydrolysis by *A. niger* GA increases by a similar value of 0.7 unit in D_2O (Selwood & Sinnott, 1990).

The pD of the D_2O buffer was measured using a common combination glass electrode with a correction applied to the observed pH meter reading to account for the solvent isotope effect on the electrode response according to eq 2 (Salomaa et al., 1964).

$$\text{pD} = \text{observed pH meter reading} + 0.4 \qquad (2)$$

The D_2O buffers were kept in sealed bottles under vacuum after preparation to minimize exposure to atmospheric moisture and used within 4 h after preparation. Care was taken to minimize exposure to atmosphere during the preparation and use, although brief exposures do not sensibly alter the percent D_2O (Quinn & Sutton, 1991).

Steady-State Kinetics. Protein concentrations were determined spectrophotometrically at 280 nm using extinction coefficients of $\epsilon_m = 1.37 \times 10^5\ M^{-1}\ cm^{-1}$ and $\epsilon_m = 1.31 \times 10^5\ M^{-1}\ cm^{-1}$, respectively, for wild-type and Trp120 → Phe GA (Clarke & Svensson, 1984; Sierks et al., 1989). The reaction rates for maltose and GF hydolysis by GA were determined by monitoring the concentration of the released glucose determined using the glucose oxidase method (Natarajan & Sierks, 1996). The steady-state kinetic data were obtained using eight substrate concentrations ranging

from 8 times above to 8 times below K_m. The Michaelis−Menten kinetic parameters, k_{cat} and K_m, were obtained by nonlinear regression of initial rates vs substrate concentration using Grafit (Leatherbarrow, 1992).

Steady-state kinetic assays of wild-type GA with maltose were performed essentially as descibed (Frandsen et al., 1994) at 45 °C in H_2O and D_2O buffers. The final enzyme concentration in the reaction mixture in these assays was 0.01 μM.

Steady-state kinetic assays of GF hydrolysis by wild-type and Trp120 → Phe GAs were conducted at 8 °C in H_2O buffer. GF substrate samples were found to contain about 5% glucose just prior to the assay. The concentrations of wild-type and Trp120 → Phe GAs in the reaction mixture, chosen to ensure that the glucose concentration did not exceed 10% of the initial GF concentration during the course of the assay, were in the 0.02−0.2 μM range.

Stopped-Flow Fluorescence Kinetics. The transient kinetics of GA reactions were investigated by monitoring the changes in the intrinsic protein fluorescence. The experiments were performed using a Hi-Tech Scientific SF-61MX multimixing stopped-flow spectrofluorometer. A 75-W xenon arc lamp from Hamamatsu was used as a light source. An excitation wavelength of 280 nm, set using a monochromator, was used with a 5-mm slit width. Light emerging out of the reaction mixture in the flow cell was passed through a cutoff emission filter (WG 320; 85% transmission at 320 nm) to resolve the fluorescence emission from the scattered excited light. The kinetics of the reaction between wild-type GA and maltose and between Trp120 → Phe GA and maltotriose in H_2O and D_2O buffers were studied at 8 °C.

Preliminary results (data not shown) indicated that observable first-order rates for Trp120 → Phe GA/maltose interactions far exceed 1000 s^{-1} at high saturating concentrations of maltose. Since first-order rates exceeding 1000 s^{-1} cannot be accurately determined using the available equipment, the Trp120 → Phe GA/maltose kinetics could not be utilized to study solvent isotope effects. However, unlike with wild-type GA, where the first-order rate constant obtained with maltotriose is faster than with maltose, the first-order rate constant for the Trp120 → Phe GA/maltotriose reaction is much slower (Olsen et al., 1993). Therefore maltose was used as a substrate to study solvent isotope effects on wild-type GA and maltotriose with Trp120 → Phe GA.

A series of stopped-flow experiments were performed by rapidly mixing equal volumes of wild-type or Trp120 → Phe GA, to a final concentration of 3 μM, with the appropriate ligand solution, and the time course of the intrinsic fluorescence intensity, as a voltage signal, was recorded. The fluorescence intensities thus acquired were compared with that of just the enzyme mixed with the relevant buffers to generate the time profile of the intrinsic fluorescence of the system. All enzyme, substrate, and buffer solutions were filtered through a 0.45-μm filter before use. The dead time of the instrument was 1 ms under the conditions used in these experiments, and mixing was achieved in less than 1 ms. The temperature was maintained at 8.0 ± 0.1 °C with a circulating water bath. In each experiment at least 512 pairs of data were collected and a minimum of four data sets were averaged for each substrate concentration. Each averaged data set was then fitted to a number of nonlinear analytical equations using the Hi-Tech rapid kinetics software. The regression analysis used is based on the Gauss−Newton method.

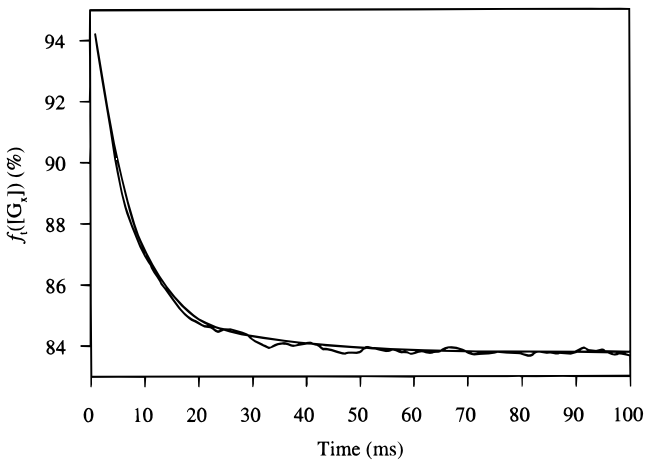

FIGURE 1: Typical stopped-flow time profile of the intrinsic enzyme fluorescence during GA reaction, shown here using wild-type GA (3 μM) reaction with maltose (0.5 mM) at 8 °C, pH 4.5, as a representative example. The intrinsic molar fluorescence of the free enzyme is arbitrarily assigned a value of 100%. The excitation wavelength was 280 nm. The signal represents fluorescence emission above 320 nm. The signal was fitted to a single-exponential curve (eq 3).

RESULTS AND DISCUSSION

Stopped-Flow Traces of GA Reactions. Wild-type and Trp120 → Phe GA reactions typically yielded stopped-flow traces, as shown in Figure 1. Only one relaxation was observed and the data were best fit to a single-exponential curve at all substrate concentrations employed. The equation of the single-exponential curve is written in the following form to facilitate mathematical analysis of the fluorescence signals:

$$f_t([G_x]) = A([G_x])\alpha([G_x]) \exp(-k_{obs}t) + f_\infty([G_x]) \quad (3)$$

where $f_t([G_x])$ represents the average molar fluorescence (i.e., total fluorescence/total number of moles) at substrate concentration $[G_x]$ and time t, $A([G_x])\alpha([G_x])$ represents the amplitude of the observable phase of the reaction, $f_\infty([G_x])$ is the average molar fluorescence at steady state, and k_{obs} is the observed first-order rate constant. Values for the amplitude, k_{obs}, and f_∞ were obtained at each substrate concentration by fitting the experimental signal to eq 3. Both the amplitude and the steady-state fluorescence are functions of substrate concentration. The amplitude is written as the product of two substrate concentration-dependent but time-independent constants, $A([G_x])$ and $\alpha[G_x])$, so the relative intrinsic fluorescence of the enzyme species could be related to trends in the signal amplitudes.

Pre-Steady-State Fluorescence Analysis of GA Reaction. The concentration dependence of the observed first-order rate constant, k_{obs}, of both wild-type GA/maltose (Figure 2) and Trp120 → Phe GA/maltotriose reactions (Figure 3) in either H_2O or D_2O is hyberbolic. The hyberbolic behavior of k_{obs} on $[G_x]$ negates the possibility of a simple one-step mechanism such as in Scheme 1a, where a linear dependence would be observed (i.e., $k_{obs} = k_1[G_x] + k_{-1}$), but rather is consistent with a two-step mechanism such as in Scheme

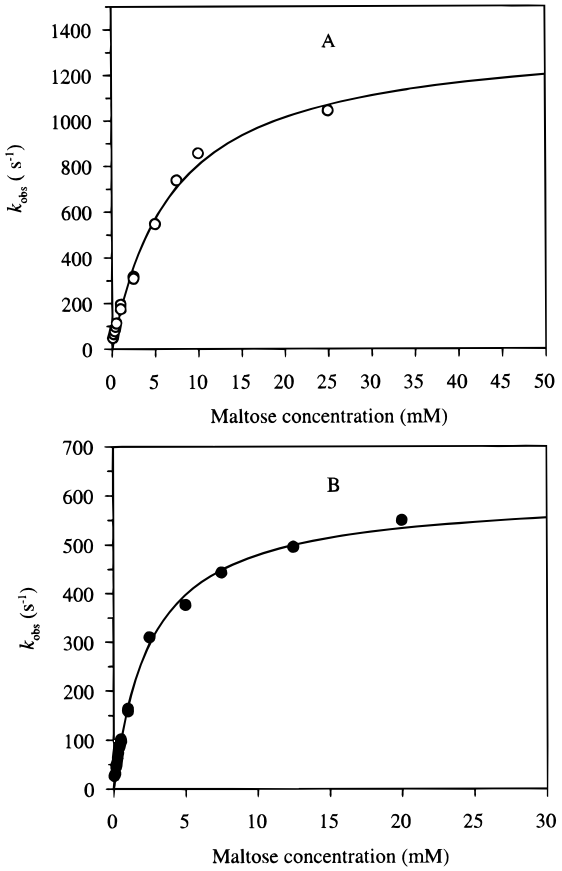

FIGURE 2: Dependence of the observed first-order rate constant, k_{obs} (eqs 3 and 10), on substrate concentration for wild-type GA reaction with maltose at 8 °C in (A) H_2O, pH 4.5, and (B) D_2O, pD 5.0. The curves were obtained by fitting experimental data to eq 7. Maximum relative standard deviations for k_{obs} data were ±8%.

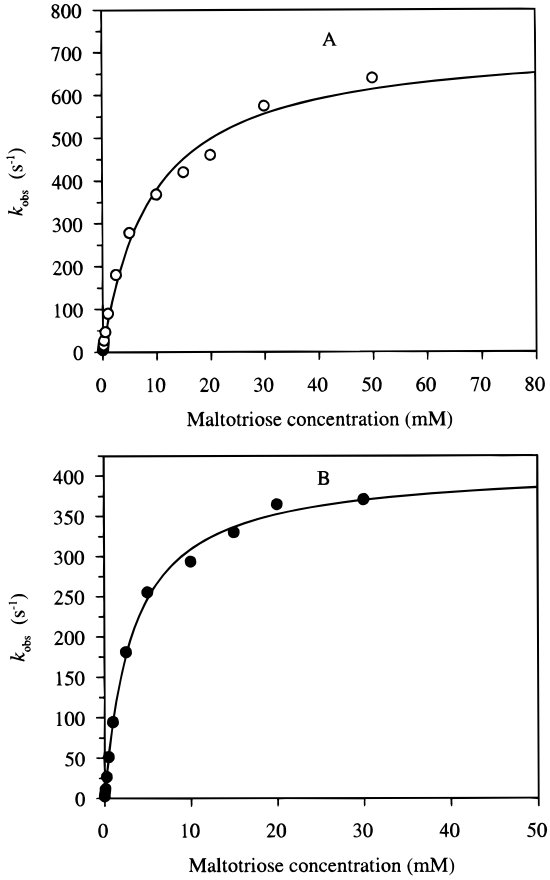

FIGURE 3: Dependence of the observed first-order rate constant, k_{obs} (eqs 3 and 10), on substrate concentration for Trp120 → Phe GA reaction with maltotriose at 8 °C in (A) H_2O, pH 4.5, and (B) D_2O, pD 5.0. The curves were obtained by fitting experimental data to eq 7. Maximum relative standard deviations for k_{obs} data were ±8%.

1b (Bagshaw et al., 1974). Scheme 1b represents a spontaneous equilibrium achieved between free enzyme (E) and the first enzyme complex (EG_x), followed by a unimolecular transformation of EG_x to the second enzyme complex (EG_x*). This means the first substrate binding step attains equilibrium on a time scale much smaller than the following unimolecular rearrangement step. Although the attainment of equilibrium in the first step is too fast to be detected by an instrument with a dead time of 1 ms, this does not imply that fluorescence is not quenched by the formation of EG_x.

Scheme 1: Pre-Steady-State Model

$$E + G_x \underset{k_{-1}}{\overset{k_1}{\rightleftharpoons}} EG_x \qquad K_1 = \frac{k_1}{k_{-1}} = \frac{[EG_x]}{[E][G_x]} \qquad \text{(a)}$$

$$E + G_x \overset{K_1}{\rightleftharpoons} EG_x \underset{k_{-2}}{\overset{k_2}{\rightleftharpoons}} EG_x^* \qquad K_1 = \frac{[EG_x]}{[E][G_x]}$$

$$K_2 = \frac{k_2}{k_{-2}} = \frac{[EG_x^*]}{[EG_x]} \qquad \text{(b)}$$

Rigorous mathematical analysis of the amplitude of the signal and the amount of fluorescence quenched provides valuable mechanistic information about the reaction which cannot be obtained just from the rate of quenching data (k_{obs}). Such an analysis enables the individual fluorescence of the involved enzyme intermediates, relative to the free enzyme, to be determined and also provides an independent alternate method to calculate equilibrium constants using fluorescence levels at steady state, f_∞. Comparison of equilibrium constants obtained by monitoring the intrinsic fluorescence of the enzyme species in the pre-steady state and by the analysis of the product formation in the steady state provides a check for the consistency of the proposed model. Equations to analyze the pre-steady-state fluorescence signals of GA reactions (Scheme 1b) will be developed in this section.

The total fluorescence of the system at any time during the reaction (eq 3) is due to the sum of the individual contributions of the different enzyme species. The total fluorescence can be expressed in terms of the individual fluorescence of each enzyme species and its concentration in the reaction mixture, thereby providing a physical significance to the terms in eq 3. The total fluorescence, which can be found experimentally, along with the calculated concentrations of all enzyme species can be used to evaluate the individual fluorescence of the enzyme-bound intermediates.

Assuming rapid equilibrium in the first step, the concentrations of all the enzyme species as a function of time can be obtained by solving enzyme mass balance equations and the individual rate equations for all involved species simultaneously. In deriving these equations, the substrate concentration $[G_x]$ is assumed to be constant since it is in excess of total enzyme concentrations, $[E_0]$ (at least 20-fold). The molar ratio of each enzyme species to total enzyme concentration is given by

$$\frac{[E]}{[E_0]} = \frac{1 - \alpha[1 - \exp(-k_{obs}t)]}{1 + K_1[G_x]} \quad (4)$$

$$\frac{[EG_x]}{[E_0]} = \frac{K_1G_x(1 - \alpha[1 - \exp(-k_{obs}t)])}{1 + K_1[G_x]} \quad (5)$$

and

$$\frac{[EG_x^*]}{[E_0]} = \alpha[1 - \exp(-k_{obs}t)] \quad (6)$$

where

$$k_{obs} = \frac{k_2[G_x]}{(1/K_1) + [G_x]} + k_{-2} \quad (7)$$

and

$$\alpha = \frac{K_1K_2[G_x]}{1 + K_1[G_x] + K_1K_2[G_x]} \quad (8)$$

The average molar fluorescence at any time t, f_t, can be expressed as a sum of the fluorescence contribution of each enzyme species as follows:

$$f_t = f_E\frac{[E]}{[E_0]} + f_{EG_x}\frac{[EG_x]}{[E_0]} + f_{EG_x^*}\frac{[EG_x^*]}{[E_0]} \quad (9)$$

where f_E, f_{EG_x}, and $f_{EG_x^*}$ are the molar fluorescence of [E], [EG_x], and [EG_x*], respectively. f_t can be written, using the expressions for the concentrations of the three enzyme species (eqs 4−6), as

$$f_t = \left[\frac{f_E + f_{EG_x}(K_1[G_x])}{1 + K_1[G_x]} - f_{EG_x^*}\right]\alpha\exp(-k_{obs}t) + \frac{f_E + f_{EG_x}(K_1[G_x])}{1 + K_1[G_x]}(1 - \alpha) + f_{EG_x^*}\alpha \quad (10)$$

Note that eq 10 is in the same form as eq 3 to which all the experimental data were fit. By comparing eq 3 with eq 10, the steady-state fluorescence, f_∞, and the $A[G_x]$ part of the amplitude of the signal can be expressed as

$$f_\infty = \frac{f_E + f_{EG_x}(K_1[G_x])}{1 + K_1[G_x]}(1 - \alpha) + f_{EG_x^*}\alpha \quad (11)$$

$$A([G_x]) = \frac{f_E + f_{EG_x}(K_1[G_x])}{1 + K_1[G_x]} - f_{EG_x^*} \quad (12)$$

The first binding step as depicted in Scheme 1b, $E + G_x \rightleftarrows EG_x$, is assumed to attain spontaneous equilibrium, meaning at time $t = 0$, equilibrium has been established. Although this is not a realistic assumption at low substrate concentrations when $K_1[G_x] \ll 1$, at high substrate concentrations when $K_1[G_x] \gg 1$, it is valid. The fluorescence at time $t = 0$, f_0, can be determined by extrapolating the observed fluorescence signal back to time $t = 0$. An expression for f_0 at any substrate concentration can be obtained by substituting $t = 0$ in eq 10 and is given by

$$f_0 = \frac{f_E + f_{EG_x}(K_1[G_x])}{1 + K_1[G_x]} \quad (13)$$

The theoretical expressions for f_0 (eq 13) and f_∞ (eq 11) can be further modified to yield equations for the percentage of fluorescence quenched in the first step (ΔF_0) and the percentage of overall fluorescence quenched at steady-state (ΔF_∞). The values for ΔF_0 and ΔF_∞, at each substrate concentration, can be experimentally determined as illustrated in Figure 4. The theoretical expressions for ΔF_0 and ΔF_∞ can be used, with the experimentally determined values, to obtain the fluorescence of the individual enzyme species, f_{EG_x} and $f_{EG_x^*}$ (relative to f_E) and the apparent dissociation constant, $1/K_1(1 + K_2)$ (discussed later).

The amount of fluorescence quenched when the reaction reaches a steady state can be obtained by subtracting f_∞ from the fluorescence of the free enzyme, f_E. The percentage of the fluorescence intensity quenched at steady state relative to the free enzyme, $\Delta F_\infty([G_x])$, is given by

$$\Delta F_\infty = \left(\frac{f_E - f_\infty}{f_E}\right)100 \quad (14)$$

ΔF_∞ can be written, using the expression for f_∞ from eq 11, as

$$\Delta F_\infty([G_x]) = \frac{\Delta F_{max}[G_x]}{\frac{1}{K_1(1 + K_2)} + [G_x]} \quad (15)$$

where the term ΔF_{max}, defined as the percentage maximum fluorescence quenched relative to free enzyme at saturating substrate concentrations, is

$$\Delta F_{max} = \left(\frac{f_E - (f_t)_{max}}{f_E}\right)100 = \frac{\left(\frac{f_E - f_{EG_x}}{f_E}\right)100 + K_2\left(\frac{f_E - f_{EG_x^*}}{f_E}\right)100}{1 + K_2} \quad (16)$$

The expression for ΔF_{max} can be simply written as

$$\Delta F_{max} = \frac{(\Delta F_{EG_x})_{max} + K_2(\Delta F_{EG_x^*})_{max}}{1 + K_2} \quad (17)$$

where $(\Delta F_{EG_x})_{max}$ and $(\Delta F_{EG_x^*})_{max}$ are the percentage differences in the fluorescence of a molecule of EG_x and EG_x*, respectively, relative to a molecule of E. The ΔF_{max} value can be determined by fitting ΔF_∞ and corresponding $[G_x]$ values to eq 15.

The fluorescence quenched at time $t = 0$, when the first binding step is at equilibrium, can similarly be determined by subtracting f_0 (eq 13) from the fluorescence of that of the free enzyme, f_E. The percentage of the fluorescence intensity quenched relative to that of free enzyme at $t = 0$, ΔF_0, can be written using the expression for f_0 from eq 13 as

$$\Delta F_0([G_x]) = \left(\frac{f_E - f_0}{f_E}\right)100 = \frac{(\Delta F_{EG_x})_{max}[G_x]}{(1/K_1) + [G_x]} \quad (18)$$

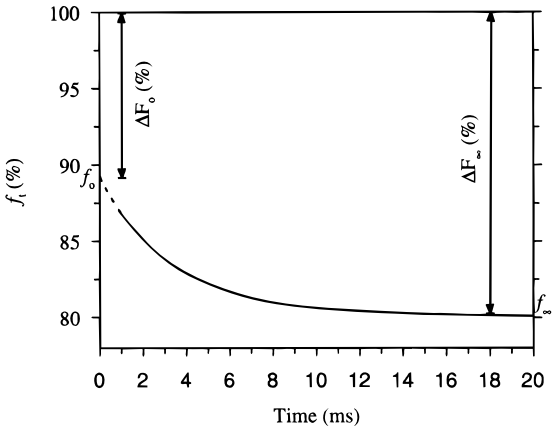

FIGURE 4: Schematic illustration of the calculation of the amount of fluorescence quenched in the first step, ΔF_0, and total fluorescence quenched, ΔF_∞, in the GA reaction, from experimental signal. The intrinsic molar fluorescence of the free enzyme is arbitrarily assigned a value of 100%. The solid line represents the typical single-exponential fluorescence signal (as described by eq 3) observed in the GA reaction where the steady-state fluorescence is denoted by f_∞. The dotted line is an interpolation of this exponential signal betweeen 0 and 1 ms (dead time). The fluorescence when the first step attains equilibrium is given by the interpolated value at $t = 0$ and is denoted by f_0. ΔF_0 is equal to the difference between the free enzyme fluorescence and f_0. ΔF_∞ is equal to the difference between free enzyme fluorescence and f_∞.

The $(\Delta F_{EG_x})_{max}$ value can be obtained by fitting $[G_x]$ and the corresponding ΔF_0 to eq 18. ΔF_{max} and $(\Delta F_{EG_x})_{max}$ values thus evaluated can be used along with the independently determined equilibrium constant K_2 (described in the following section) in eq 17 to obtain $(\Delta F_{EG_x*})_{max}$. Thus the molar fluorescence of both the enzyme intermediates, EG_x and EG_x*, relative to that of the free enzyme can be determined.

Determination of Rate Constants. The stopped-flow fluorescence traces obtained for GA reactions were fit to eq 3 at various substrate concentrations to generate a k_{obs} vs $[G_x]$ profile. k_{obs} is a measure of the rate of production of EG_x* as seen from eq 6. The association constant, K_1, and intrinsic rate constants, k_2 and k_{-2}, were determined by fitting k_{obs} vs $[G_x]$ data to eq 7. At low substrate concentrations (when $[G_x] \ll 1/K_1$), eq 7 reduces to the following linear relationship between k_{obs} and $[G_x]$: $k_{obs} = K_1k_2[G_x] + k_{-2}$. k_{-2} values were thus determined as the ordinate intercept of such a plot. K_1 and k_2 were determined by fitting $(k_{obs} - k_{-2})$ values to eq 7. The K_1, k_2, and k_{-2} values thus determined for wild-type GA/maltose and Trp120 → Phe GA/maltotriose reactions in H_2O and D_2O are given in Table 1.

Fluorescence Quenching in the Individual Steps. The magnitude of the fluorescence changes observed during the GA reactions can be used first to qualitatively recognize the relative fluorescence intensity of the enzyme species and second to quantitatively determine the molar fluorescence of these enzyme intermediates, relative to free enzyme, based on fitting experimental data to theoretical equations. A qualitative analysis based on trends in the fluorescence changes can be used for reactions where data are not available throughout the entire range of substrate concentrations, offering an elegant method to identify the fluorescence levels of enzyme intermediates. When comprehensive data can be obtained, the qualitative analysis can be used to complement the quantitative fluorescence analysis. In this section we will provide methods, using the equations developed in the previous section, for both qualitative and quantitative fluorescence analyses.

Trends in the amplitude of the observed signal, which have often been overlooked in pre-steady-state spectrophotometric analyses, can be used to qualitatively recognize the relative magnitude of the fluorescence intensities of different intermediates in the reaction. Analysis of the fluorescence observed indicated that the amplitude of the signal clearly decreases with increasing substrate concentrations for both wild-type and Trp120 → Phe GA reactions. The amplitudes of the signal in the wild-type GA/maltose reaction, for instance, are 9.1% and 5.9% for substrate concentrations of 2.5 and 7.5 mM, respectively, as illustrated in Figure 5. The amplitude of the fluorescence signal is represented by the expression $A([G_x])\alpha$, where $A([G_x])$ and α are defined in eqs 12 and 8, respectively. α monotonically increases with increasing substrate concentrations, so in order for the amplitude of the signal to decrease, $A([G_x])$ has to decrease with increasing substrate concentration. However, according to differential calculus, $A([G_x])$ can decrease with increasing substrate concentration only if $f_{EG_x} < f_E$. If $f_{EG_x} = f_E$, as implicitly assumed in earlier analyses (Olsen et al., 1992, 1993), then $A([G_x])$ would be concentration-independent, which contradicts the experimental data obtained here. Therefore, this qualitative analysis clearly shows that fluorescence is quenched in the formation of the first enzyme−substrate complex (i.e., $f_{EG_x} < f_E$).

The magnitude of f_{EG_x} relative to f_{EG_x*}, can also be determined by examining the $A([G_x])$ term at extremely low and high substrate concentrations. If $f_{EG_x} > f_{EG_x*}$, then the

Table 1: Pre-Steady-State and Steady-State Kinetic Results of the Wild-Type and Trp120 → Phe GA Reactions at 8 °C

	wild-type GA-maltose		Trp120 → Phe GA-maltotriose	
reaction buffer	H_2O[a]	D_2O[b]	H_2O[a]	D_2O[b]
K_1 (mM^{-1})	0.12 ± 0.01	0.32 ± 0.01	0.11 ± 0.01	0.30 ± 0.02
k_2 (s^{-1})	1392 ± 68	606 ± 9	727 ± 29	410 ± 7
k_{-2} (s^{-1})	31.7 ± 1.9	16.5 ± 1.7	1.94 ± 0.30	1.10 ± 0.07
ΔF_{max} (%)	20.6 ± 0.4	23.1 ± 0.3	16.9 ± 0.2	18.0 ± 0.2
$(\Delta F_{EG_x})_{max}$ (%)	16.2 ± 0.5	19.9 ± 0.5	12.7 ± 0.3	15.8 ± 1.1
$(\Delta F_{EG_x*})_{max}$ (%)	20.7 ± 0.4	23.2 ± 0.3	16.9 ± 0.2	18.1 ± 0.2
K_d[c] (mM)	0.182 ± 0.040	0.082 ± 0.010	0.025 ± 0.004	0.009 ± 0.001
K_d[d] (mM)	0.161 ± 0.020	0.142 ± 0.011	0.014 ± 0.002	0.010 ± 0.001
K_m[e] (mM)	0.180 ± 0.020	nd[f]	0.044 ± 0.005	nd
k_{cat}[e] (s^{-1})	0.33 ± 0.01	nd	0.034 ± 0.001	nd

[a] pH 4.5. [b] pD 5.0. [c] K_d calculated substituting K_1, k_2, and k_{-2} in eq 19. [d] K_d calculated from fluorescence quenching data using eq 15. [e] From Olsen et al. (1993). [f] Not determined.

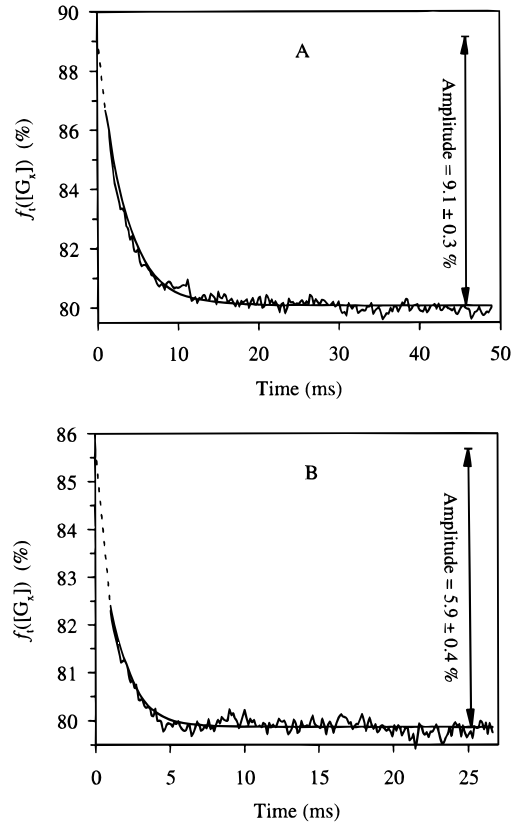

FIGURE 5: Illustration of the decrease in the amplitude of the observed fluorescence signal with increasing substrate concentrations in GA reactions. The amplitudes of the fluorescence signal in the wild-type GA (3 μM) reaction in H_2O with maltose at substrate concentrations of (A) 2.5 mM and (B) 7.5 mM are shown here as examples. The magnitude of the intrinsic molar fluorescence of the system are all relative to that of the free enzyme (100%). The curves are a fit of the stopped-flow traces to eq 3, with the solid curve representing the fit to the experimentally observed signal and the dotted curve representing the interpolation of the data between 0 and 1 ms (dead time). The amplitude, $A[G_x]\alpha$, is as defined in eq 3 and is simply equal to the difference in the intrinsic enzyme fluorescence at times $t = 0$ and time $t = \infty$ [or times at which $\exp(-k_{obs}*t)$ is negligible].

amplitude of the fluorescence signal should stay positive for all the substrate concentrations. If $f_{EG_x} < f_{EG_x*}$, then the amplitude of the signal should be positive (i.e., $f_t \geq f_\infty$) for substrate concentrations at which $K_1[G_x] \ll 1$ and negative (i.e., $f_t \leq f_\infty$) at substrate concentrations at which $K_1[G_x] \gg 1$. In analyzing the GA reaction data, the amplitude of the signals were always positive except for one point at the highest substrate concentration utilized (75 mM, $K_1[G_x] = 9$) in the wild-type GA reaction with maltose in H_2O where a signal with a small but negative amplitude was observed. Although this indicates that f_{EG_x} should be less than f_{EG_x*}, this one experimental point should be dealt with cautiously since this phenomenon was observed at a concentration which is excessively higher than the concentrations which are typically used to study GA hydrolysis. At this high substrate concentration, multiple substrate binding is known to occur (Nikolov et al., 1989). The relative magnitudes of f_{EG_x} and f_{EG_x*}, therefore, cannot be resolved with certainty with such a qualitative analysis due to the lack of experimental data and competing effects at high substrate concentrations. The magnitudes of f_{EG_x} and f_{EG_x*}, relative to that of f_E, however, can still be determined by the following quantitative analysis.

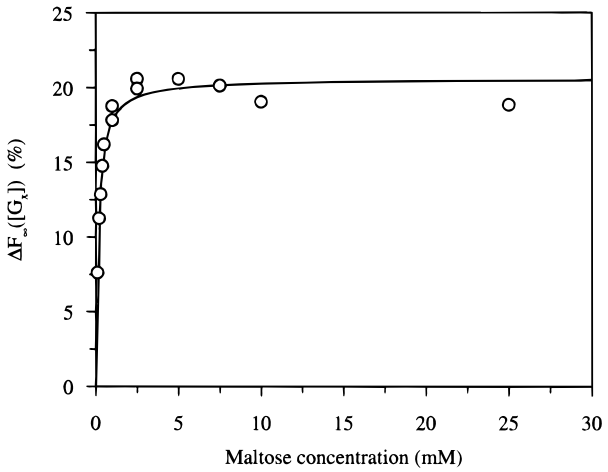

FIGURE 6: Relative fluorescence intensity decrease obtained when the wild-type GA (3 μM) reaction with maltose in H_2O apparently reaches a steady state, $\Delta F_\infty([G_x])$, plotted against substrate concentration. ΔF_∞ values are calculated from the experimental signal as described in Figure 4. Reaction conditions: pH 4.5, 8 °C. The curve is a fit of the experimental values of $\Delta F_\infty([G_x])$ to eq 15. Relative standard deviation for $\Delta F_\infty([G_x])$ data is ±1%.

A typical plot of the concentration dependence of ΔF_∞ on $[G_x]$ for all GA reactions studied in this work is illustrated in Figure 6, showing the fluorescence data of wild-type GA/maltose in H_2O. The percentage of the total fluorescence quenched, $\Delta F_\infty([G_x])$, at different substrate concentrations (as illustrated in Figure 4) for the wild-type GA/maltose and Trp120 → Phe GA/maltotriose reactions in H_2O and D_2O were fit to eq 15 and the constant ΔF_{max} thus obtained are given in Table 1. The values of $1/[K_1(1 + K_2)]$ were also obtained from the same fit and are given in Table 1 as K_d, the apparent dissociation constant, shown to be equivalent in eq 19. K_d, representing the overall dissociation constant of all enzyme-bound species, for the reaction in Scheme 1b can be calculated from the relationship

$$K_d = \frac{[E][G_x]}{[EG_x] + [EG_x*]} = \frac{1}{K_1(1 + K_2)} \qquad (19)$$

The value of $1/[K_1(1 + K_2)]$ obtained from the fluorescence data provides a direct way of determining K_d. An alternative way of calculating K_d is by substituting the rate constants, obtained from the k_{obs} data fit to eq 7, in eq 19. The K_d values (Table 1) determined from the fluorescence quenching data and also from the independently calculated rate constants using eq 19, are in good agreement (within 10−75% of each other) for both wild-type and Trp120 → Phe GA reactions, indicating the model is internally consistent. K_d values determined this way also provide a link between pre-steady-state and steady-state kinetic parameters, the significance of which will be discussed shortly.

The percentage of fluorescence quenched when the first step reaches equilibrium, $\Delta F_0[G_x]$, was calculated for both wild-type/maltose and Trp120 → Phe GA/maltotriose reactions in H_2O and D_2O for all substrate concentrations (as described in Figure 4). A plot of resultant ΔF_0 values vs $[G_x]$ is shown in Figure 7 for the wild-type GA/maltose reaction in H_2O as an illustrative example. $\Delta F_0[G_x]$ values were fitted to eq 18 to obtain $(\Delta F_{EG_x})_{max}$ for each reaction (values shown in Table 1). K_1 values can also be obtained from such a fit but are not very reliable because the

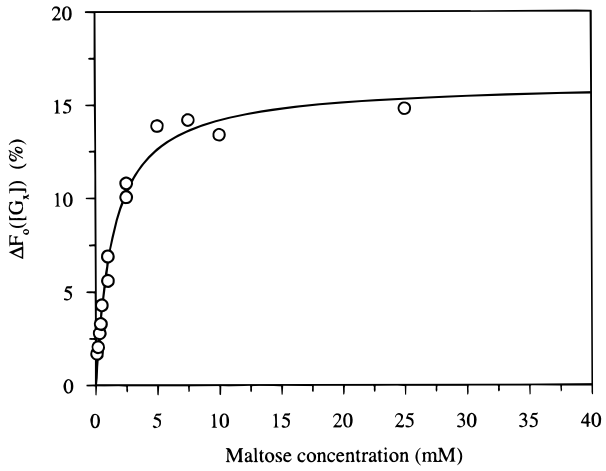

FIGURE 7: Apparent relative fluorescence intensity decrease obtained during the spontaneous GA/substrate binding step $\Delta F_0([G_x])$, plotted against substrate concentration. ΔF_0 values are calculated from the experimental signal as described in Figure 4. The magnitude of fluorescence of wild-type GA quenched at different concentrations of maltose is shown here as an example. Reaction conditions: pH 4.5, 8 °C. The curve is a fit of the experimental values of $\Delta F_0([G_x])$ to eq 18. Relative standard deviation for $\Delta F_0([G_x])$ data is ±4%.

assumption of a spontaneous equilibrium, though practical, is not very realistic at low substrate concentrations. Assumption of spontaneous equilibrium at low substrate concentrations will result in a slight underestimation of the amount of quenching in the first step. This underestimation, in turn, will result in a lower $1/K_1$ value. Slightly lower $1/K_1$ values obtained from ΔF_0 vs $[G_x]$ fits (data not shown) compared to the $1/K_1$ values calculated from k_{obs} data for both wild-type and Trp120 → Phe GA reactions support this argument. In contrast, determination of $(\Delta F_{EG_x})_{max}$, which is equal to the fluorescence quenched in the first step at saturating substrate concentration, is relatively insensitive to slight inaccuracies in the estimated ΔF_0 values at low substrate concentrations since ΔF_0 (Figure 7) clearly approaches a constant value at the higher concentrations employed in the study. The calculated $(\Delta F_{EG_x})_{max}$ values were then substituted into eq 17 to determine $(\Delta F_{EG_x*})_{max}$ (Table 1). The individual fluorescence of the enzyme-bound intermediates, EG_x and EG_x*, relative to that of the free enzyme in GA reactions can therefore be determined. $(\Delta F_{EG_x})_{max}$ is less than $(\Delta F_{EG_x*})_{max}$ for both wild-type and Trp120 → Phe GA reactions, indicating that the fluorescence is quenched in the unimolecular step (i.e., $f_{EG_x} > f_{EG_x*}$). The one experimental observation of small but negative amplitude observed in wild-type GA/maltose reaction in H_2O at an excessively high concentration of maltose, suggesting that $f_{EG_x} < f_{EG_x*}$, therefore is very likely due to multiple substrate binding, as suggested earlier. The analysis presented here is limited to single substrate binding.

Individual Steps in GA Mechanism. The steady-state kinetic parameters k_{cat} and K_m and the pre-steady-state constants K_1, k_2, and k_{-2} for wild-type GA/maltose and Trp120 → Phe GA/maltotriose reactions in H_2O and D_2O are presented in Table 1. The pre-steady-state kinetic results indicate that the first two steps of the GA reaction represent an enzyme−substrate association followed by a unimolecular reconfiguration (Scheme 1b). Since the fluorescence signal reaches a steady intensity after these two steps have apparently equilibrated, it is reasonable to assume that the rate-limiting step of the GA reaction immediately follows the unimolecular rearrangement step. A reaction model involving these steps, as depicted in Scheme 2, can be used to account for GA reactions. A similar model has been previously applied for *R. niveus* (Tanaka, 1982) and *A. niger* GA (Olsen et al., 1992, 1993) reactions, although in this work the identification of the enzyme-bound intermediates, EG_x and EG_x*, and their fluorescence contributions are different.

Scheme 2: Reaction Model in Development

$$E + G_x \underset{k_{-1}}{\overset{k_1}{\rightleftharpoons}} EG_x \underset{k_{-2}}{\overset{k_2}{\rightleftharpoons}} EG_x* \xrightarrow[\text{slowest step}]{k_3}$$

The steady-state kinetic parameters, k_{cat} and K_m, for the reaction model described in Scheme 2 can be expressed in terms of microscopic rate constants using the Briggs−Haldane steady-state approximation as shown previously (Olsen et al., 1993):

$$k_{cat} = \frac{k_2 k_3}{k_2 + k_{-2} + k_3} \tag{20}$$

$$K_m = \frac{k_{-1}(k_{-2} + k_3) + k_2 k_3}{k_1(k_2 + k_{-2} + k_3)} \tag{21}$$

The k_{cat} and $K_m$values determined using steady-state kinetics and the K_1, k_2 and k_{-2} values determined using pre-steady-state kinetics can be linked using eqs 20 and 21 to obtain a complete picture of the GA reaction. For both wild-type GA/maltose and Trp120 → PheGA/maltotriose reactions, $k_{-2} \ll k_2$ and $k_{cat} \ll k_2$, so eq 20 reduces to

$$k_{cat} = \frac{k_2 k_3}{k_2 + k_{-2} + k_3} \approx k_3 \tag{22}$$

Thus the rate of the slowest step of the GA reaction is equal to the catalytic turnover of the enzyme. Recent studies indicate release of the reducing-end sugar is the rate-limiting step in the GA mechanism (Sierks & Svensson, 1996; Natarajan & Sierks, 1996), which would imply that EG_x* is an enzyme−product complex dissociating with a rate equal to k_3.

Equation 21 can be simplified similarly to

$$K_m = \frac{k_{-1}(k_{-2} + k_3) + k_2 k_3}{k_1(k_2 + k_{-2} + k_3)} \approx K_d + \frac{k_3}{k_1} \tag{23}$$

where K_d is the overall dissociation constant for the reaction described in Scheme 1b as defined in eq 19. Equation 23 shows that K_m is always greater than or equal to K_d. Since k_1, the association rate constant for enzyme−substrate interaction, is typically in the range of 10^3−10^5 s^{-1} mM^{-1} (Fersht, 1985), the value k_3/k_1 should be relatively small compared to K_d, and the K_m values should be identical to K_d values. K_d values (Table 1) for both the wild-type and Trp120 → Phe GA reactions in H_2O are very similar to corresponding K_m values (Table 1), indicating that the three-step reaction model (Scheme 2) is essentially correct and the data do not warrant an extended mechanism with more than three steps. The GA reaction model can therefore be more specifically written as illustrated in Scheme 3, where EG_x is the productive enzyme−substrate complex, EP is the

enzyme−product complex, and dissociation of this complex is the rate-determining step.

Scheme 3: Proposed Reaction Model

$$E + G_x \underset{k_{-1}}{\overset{k_1}{\rightleftharpoons}} EG_x \underset{k_{-2}}{\overset{k_2}{\rightleftharpoons}} EP \xrightarrow{k_{cat}} E + P$$

Assuming that fluorescence was not quenched in the first step, the formation of the first enzyme complex, EG_x, was initially identified as a loose binding step (Olsen et al., 1992, 1993). Here we have rigorously shown, however, that the intrinsic fluorescence of the enzyme is primarily quenched in the first enzyme−substrate association step. The values of $(\Delta F_{EG_x})_{max}$ and $(\Delta F_{EG_x*})_{max}$ (Table 1) also indicate that the fluorescence is further quenched in the second unimolecular step. For example, in the wild-type GA/maltose reaction, the fluorescence quenching associated with just the first step, $(\Delta F_{EG_x})_{max}$, is 16.2% and the fluorescence quenching associated with both the steps, $(\Delta F_{EG_x*})_{max}$, is 20.7%. Therefore, nearly 80% of the total fluorescence quenched in going from E to EG_x* results from formation of the initial substrate complex. The fluorescence quenching in the Trp120 → Phe GA reaction with maltose would provide a valuable comparison between the wild-type and mutant enzymes, but due to the limitations of the current stopped-flow instrument technology described earlier, the reaction could not be monitored with satisfactory precision at saturating concentrations of the substrate. The Trp120 → Phe GA/maltotriose reaction, however, posed no such problems and $(\Delta F_{EG_x})_{max}$ and $(\Delta F_{EG_x*})_{max}$ values (Table 1) determined for the reaction in H_2O are 12.7% and 16.9%, respectively. Again nearly 75% of the total fluorescence quenched is attributable to formation of the initial substrate complex. However, since the wild-type and mutant GA reactions were followed using different substrates, some caution must be taken in making direct comparisons between the amount of fluorescence quenched in each case.

Since most of the fluorescence quenching observed occurs in the first enzyme−substrate complex formation with either maltose or maltotriose, it is very likely that the complex is a productive enzyme complex, contrary to the previously suggested loosely bound complex. Many Trp residues, Trp52, Trp178, Trp317, and Trp417, are situated around the general acid catalytic group Glu179 as seen from the GA crystal structure (Aleshin et al., 1994). Since two glucosyl residues occupying subsites 1 and 2 in the productive binding mode straddle Glu179 before hydrolysis occurs, the intrinsic fluorescence of the enzyme during the substrate binding step is likely to decrease due to quenching of one or more of these Trp residues around Glu179. To further explore whether EG_x* is an enzyme−product complex, the solvent isotope effect on transient kinetics of wild-type and Trp120 → Phe GA reactions were studied using D_2O.

Deuterium Solvent Isotope Effects on Pre-Steady-State Kinetics. The ratio of the value of the equilibrium constant (K_1) for the first step for wild-type GA/maltose reactions obtained in D_2O and H_2O is 2.7 (Table 1). The GA active site−substrate interactions are characterized by extensive hydrogen bonding involving all hydroxyl groups around the first and the second subsites (Aleshin et al., 1994) typical of many protein−carbohydrate interactions (Quiocho, 1986). The presence of cooperative and bidentate hydrogen bonds and the occurrence of hydrogen-bond networks is thought to confer affinity and specificity to the GA interaction (Coutinho & Reilly, 1994). The length of the hydrogen bond and hence its configuration is changed considerably upon deuterium substitution (Jencks, 1987). The effect of D_2O on K_1, the substrate association equilibrium constant, is very likely a result of significant differences in the very specific hydrogen-bonding network in the GA active site caused by changed hydrogen-bond configurations due to deuterium substitutions.

Both k_2 and k_{-2} values are substantially lower in D_2O compared to H_2O for both the wild-type and Trp120 → Phe GA reactions. The $k_2(H_2O)/k_2(D_2O)$ and $k_{-2}(H_2O)/k_{-2}/(D_2O)$ ratios are 2.3 and 1.9, respectively, for the wild-type GA/maltose reaction. Similar deuterium isotopic effects on both the forward and reverse rates suggest an occurrence of proton transfer in the second step. In an earlier study, a similar 1.8-fold decrease in k_{cat} for GA hydrolysis of *p*-nitrophenyl α-D-glucopyranoside in D_2O was observed (Selwood & Sinnott, 1990). In that study, *p*-nitrophenyl α-D-glucopyranoside was utilized since it is a poor substrate and bond-breaking was assumed to be rate-limiting so any D_2O effects could be interpreted to reflect proton tranfers in the hydrolytic step. An approximately 2-fold decrease of k_2 and k_{-2} for maltose in D_2O, similar in magnitude to the D_2O isotopic effect on proton transfers for *p*-nitrophenyl α-D-glucopyranoside, provides further evidence that the second unimolecular rearrangement step (Scheme 3) represents the hydrolytic step for oligosaccharide substrates. A proton inventory on k_{cat} for *p*-nitrophenyl α-D-glucopyranoside hydrolysis by GA indicated that the D_2O isotopic effect arises from a single proton tranfer (Selwood & Sinnott, 1990). The hydrolytic mechanism of GA has been postulated to involve an attack of the general acid residue Glu179 proton on the aglycon in concert with the reaction of the water molecule located in the active site with C-1. The proton attached to water is abstracted by Glu400, the catalytic base, resulting in the production of glucose (Figure 8) (Frandsen et al., 1994). This mechanism involves two proton transfers, the abstraction of the exchangeable proton from Glu179 by the glucosidic oxygen and the removal of a proton by Glu400 assisting solvent attack at C-1, and either one of these two protons may contribute to the observed isotopic effect.

To further probe the possibility of the second unimolecular rearrangement step being the hydrolytic step, the Trp120 → Phe GA/maltotriose reaction was studied in H_2O and D_2O. Since Trp120 does not participate directly in any of the proton transfers in the hydrolytic step and the chemistry of the hydrolytic step with maltotriose should be identical to that with maltose, we expect an isotopic effect in Trp120 → Phe GA/maltotriose reactions similar to that observed with wild-type GA/maltose reactions. Similar to wild-type GA, a 2.7-fold increase in the K_1 value was observed. A similar effect to that of wild-type GA was also seen in the second step with the mutant enzyme, where both $k_2(H_2O)/k_2(D_2O)$ and $k_{-2}(H_2O)/k_{-2}(D_2O)$ ratios have values of 1.8. The similar isotopic effects on k_2 and k_{-2} in both wild-type and Trp120 → Phe GA reactions with oligosaccharides strongly suggest that the second step, as indicated in Scheme 3, is the hydrolytic chemical step.

Solvent Deuterium Effects on Steady-State Kinetics. Values for the steady-state kinetic parameters, k_{cat} and K_m, determined for the wild-type GA/maltose reaction at 45 °C

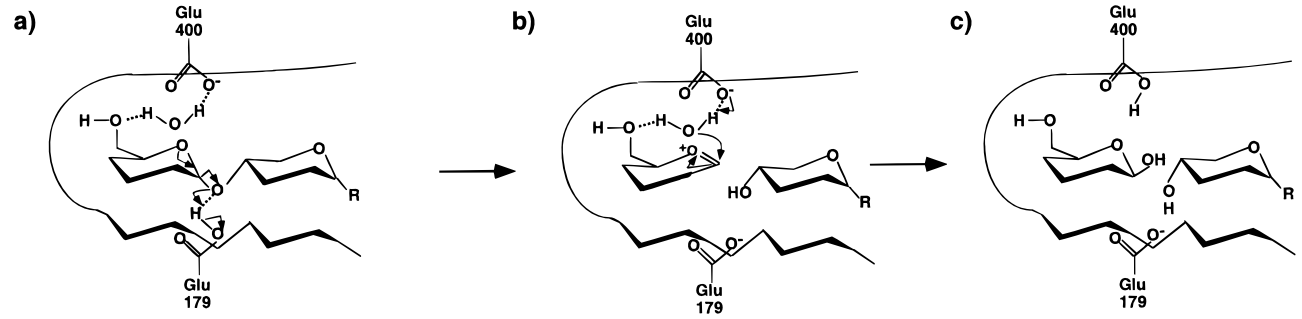

FIGURE 8: Schematic representation of the hydrolytic mechanism of glucoamylase (Frandsen et al., 1994), illustrated with oligosaccharide as substrate. The movement of electrons is indicated by arrows, and hydrogen-bond interactions are shown by dashed lines. (a) Donation of hydrogen by Glu 179, the general acid, to the oxygen of the glucosidic bond resulting in the formation of an oxocarbonium ion intermediate; (b) nucleophilic attack of water on C-1 of the aglycon moiety guided by general base Glu400, and (c) the newly formed β-D-glucose product after hydrolysis.

Table 2: Steady-State Kinetic Parameters for Maltose Hydrolysis by Wild-Type GA in H_2O and D_2O at 45 °C

solvent	H_2O[a]	D_2O[b]
k_{cat} (s^{-1})	9.2 ± 0.4	8.5 ± 0.2
K_m (mM)	1.4 ± 0.2	0.68 ± 0.06

[a] pH 4.5; from Natarajan and Sierks (1996). [b] pD 5.0.

are given in Table 2. The effect of D_2O on k_{cat} reflected by the ratio $k_{cat}(H_2O)/k_{cat}(D_2O)$ is 1.1, indicating only a very minor isotopic effect probably due to secondary effects. The absence of a significant isotope effect on the turnover rate provides additional evidence that the hydrolytic step, which should involve proton transfers from the rapidly solvent-exchangeable hydrogens, is not the rate-limiting step of the GA reaction mechanism for oligosaccharide hydrolysis. In contrast, k_{cat} for *p*-nitrophenyl α-D-glucopyranoside, a poor substrate for which bond hydrolysis is not likely to be obscured by noncovalent events, decreased significantly by a factor of 1.8 (Selwood & Sinnott, 1990). Similar turnover rates in both H_2O and D_2O for maltose also indicate that GA does not undergo any major conformational changes in D_2O, eliminating this as a potential explanation for the isotopic effects observed on k_2 and k_{-2} in pre-steady-state kinetics. The ratio $K_m(H_2O)/K_m(D_2O)$ for wild-type GA/maltose reaction is 2.1, indicating that enzyme complexes are bound better in D_2O than in H_2O. The effect on K_m may be due to the tightly formed enzyme−substrate association complexes, since a similar effect was observed on the equilbrium constant K_1. Solvent isotope effects on K_m are more the rule than the exception (Jencks, 1987), though the precise nature of the effects is not very well understood. D_2O changes hydrogen-bond and hydrophobic interactions, and though these changes are individually small, the presence of a considerable number of these interactions can result in a significant solvent deuterium effect (Schowen, 1975; Kresge, 1975). D_2O effects on the elaborate hydrogen-bonding network in the GA active site would account for the observed changes in K_1 and K_m.

GF Kinetics Probing the Importance of Release of Reducing-End Sugars. The isotope effects on both the pre-steady-state and steady-state kinetics are consistent with the reaction model depicted in Scheme 3, where the glucosidic bond hydrolysis is not the rate-limiting step of the GA mechanism. Recent evidence, based on k_{cat}/K_m determinations of wild-type GA and several GA mutants with GF and maltose, strongly suggested that the slowest step in the GA reaction with oligosaccharides is the release of the reducing-end sugars after hydrolysis (Sierks & Svensson, 1996). We determined individual k_{cat} and K_m values with wild-type GA and Trp120 → Phe GA for GF hydrolysis at 8 °C (Table 3) to complement earlier work (Natarajan & Sierks, 1996) which indicated that Trp120 loop residues played a crucial role in the rate-determining product release step. The Trp120 → Phe mutation had very little effect on the steady-state kinetic parameters for GF hydrolysis as both k_{cat} and K_m values were identical to those of wild type. In contrast, k_{cat} of Trp120 → Phe GA with maltose is 33-fold lower than that of wild-type GA. The hydrolytic ability of GA is therefore not affected by the mutation, although the product release for oligosaccharide hydrolysis is dramatically decreased. With GF, the turnover rate of wild-type GA is about 100-fold higher than with maltose, whereas for Trp120 → Phe GA it is 3600-fold higher. The large differences between these values argue against the increased activity on GF being attributable to fluoride acting as a better leaving group. Rather, these results provide additional strong evidence that the release of the reducing-end sugars is the slowest step of GA mechanism for natural oligosaccharide substrates.

Conclusion. We propose the following minimal GA mechanism based on our findings from pre-steady-state fluorescence signal analysis, deuterium solvent isotopic effects on transient and steady-state kinetics, and GF hydrolysis kinetics:

$$E + G_x \underset{k_{-1}}{\overset{k_1}{\rightleftharpoons}} EG_x \underset{k_{-2}}{\overset{k_2}{\rightleftharpoons}} EP \xrightarrow{k_{cat}} E + G_1 + \text{reducing-end product}$$

The first step represents a rapid enzyme−substrate association step leading to a productive enzyme−substrate complex, EG_x, which significantly quenches fluorescence of the tryptophans in the active site. Even though substrate binding is depicted as a one-step process in the above mechanism, it could possibly be a series of equilibrium steps consisting of a loose binding and/or substrate-induced enzyme conformational changes occurring too fast to be detected as individual steps by current stopped-flow techniques. The second step represents the glucosidic bond hydrolysis step as suggested by similar 2-fold deuterium solvent isotopic effects on both the forward and reverse rates with wild-type and Trp120 → Phe GAs. The third step represents the rate-determining product release step.

The solvent isotopic effect, though strongly suggestive, is not conclusive evidence that the second step is indeed the

Table 3: Steady-State Kinetic Parameters for Wild-Type and Trp120 → Phe GA Hydrolysis at 8 °C, pH 4.5

	wild-type GA		Trp120 → Phe GA	
enzyme	k_{cat} (s^{-1})	K_m (mM)	k_{cat} (s^{-1})	K_m (mM)
GF substrate	31.9 ± 1.2	17.1 ± 1.9	36.1 ± 1.1	17.5 ± 1.5
maltose substrate[a]	0.33 ± 0.01	0.18 ± 0.02	0.01 ± 0.0002	0.052 ± 0.003

[a] From Olsen et al. (1993).

hydrolytic step; however, a number of other independent pieces of evidence support this claim. First, K_m calculated using steady-state kinetics is very similar to K_d calculated using pre-steady-state kinetics, indicating there are no significant enzyme-bound intermediates other than those represented in Scheme 3. Second, the recovery of wild-type level activity of Trp120 → Phe GA for GF hydrolysis suggests that the rate-limiting step of GA oligosaccharide hydrolytic mechanism is the very slow release of the reducing-end product. Finally, steady-state isotopic studies indicate that a nonhydrolytic process is the rate-determining step.

The conclusion from this study is that GA reaction with oligosaccharides, contrary to general perception, is not limited by hydrolysis but by the slow product release. The realization that maltose is hydrolyzed at the rate of about 1400 s^{-1} while the products are released over 4000-fold more slowly at a rate of only about 0.3 s^{-1} at 8 °C has significant implications for tailoring GA activity. This insight into the rate-determining step increases the potential for improving GA activity as the task of devising ways to enhance product release is more realistic than to engineer an enzyme with better chemistry.

ACKNOWLEDGMENT

We are grateful to Cetus Corp. for the gift of the glucoamylase gene, yeast expression vector, and *S. cerevisiae* strain and to Dr. Alexander Scriabine (Miles Inc., West Haven, CT) for the gift of acarbose. We also thank Dr. Donald Creighton for his insightful discussions.

REFERENCES

Aleshin, A. E., Hoffman, C., Firsov, L. M., & Honzatko, R. B. (1994) *J. Mol. Biol. 238*, 575−591.

Bagshaw, C. R., Eccleston, J. F., Eckstein, F., Goody, R. S., Gutfreund, H., & Trentham, D. R. (1974) *Biochem. J. 141*, 351−364.

Clarke, A. J., & Svensson, B. (1984) *Carlsberg Res. Commun. 49*, 111−122.

Coutinho, P. M., & Reilly, P. J. (1994) *Protein Eng. 7*, 393−400.

Fersht, A. (1985) *Enzyme Structure and Mechanism*, 2nd ed., W. H. Freeman, New York.

Frandsen, T. P., Dupont, C., Lehmbeck, J., Stoffer, B., Sierks, M. R., Honzatko, R., & Svensson, B. (1994) *Biochemistry 33*, 13808−13816.

Harris, E. M. S., Aleshin, A. E., Firsov, L. M., & Honzatko, R. B. (1993) *Biochemistry 32*, 1618−1626.

Hiromi, K. (1972) in *Proteins: Structure and Function* (Funatsu, M., Hiromi, K., Imahori, K., Murachi, T., & Narita, K., Eds.) Vol. 2, pp 1−46, Halsted Press, New York.

Hiromi, K., Kawai, M., & Ono, S. (1966a) *J. Biochem. (Tokyo) 59*, 476−480.

Hiromi, K., Takahashi, K., Hamauzu, Z., & Ono, S. (1966b) *J. Biochem. (Tokyo) 59*, 476−480.

Hiromi, K., Ohnishi, M., & Tanaka, A. (1983) *Mol. Cell. Biochem. 51*, 79−85.

Jencks, W. P. (1987) *Catalysis in Chemistry and Enzymology*, pp 243−281, Dover Publications, New York.

Kitahata, S., Brewer, C. F., Genghof, D. S., Sawai, T., & Hehre, E. J. (1981) *J. Biol. Chem. 256*, 6017−6026.

Kresge, A. J. (1975) *Faraday Symp. Chem. Soc. 10*, 160−168.

Leatherbarrow, R. J. (1992) *Grafit*, Version 3.0, Erithacus Software Ltd., Staines, U.K.

Natarajan, S., & Sierks, M. R. (1996) *Biochemistry 35*, 3050−3058.

Nikolov, Z. L., Meagher, M. M., & Reilly, P. J. (1989) *Biotechnol. Bioeng. 34*, 694−704.

Olsen, K., Svensson, B., & Christensen, U. (1992) *Eur. J. Biochem. 209*, 777−784.

Olsen, K., Christiansen, U., Sierks, M. R., & Svensson, B. (1993) *Biochemistry 32*, 9686−9693.

Quinn, M. D., & Sutton, L. D. (1991) in *Enzyme Mechanism from Isotope Effects* (Cook, P. F., Ed.) pp 73−126, CRC Press, Boca Raton, FL.

Quiocho, F. (1986) *Annu. Rev. Biochem. 55*, 287−315.

Salomaa, P., Schaleger, L. L., & Long, F. A. (1964) *J. Am. Chem. Soc. 86*, 1−8.

Schowen, R. L. (1975) *Faraday Symp. Chem. Soc. 10*, 160−168.

Schowen, R. L. (1976) in *Isotope Effects on Enzyme-Catalyzed Reactions* (Cleland, W. W., O'Leary, M. H., & Northrop, D. B., Eds.) pp 65−99, University Park Press, Baltimore, MD.

Selwood, T., & Sinnott, M. L. (1990) in *Molecular Mechanisms in Biorganic Processes* (Golding, B. T., & Bleasdale, C., Eds.) Royal Society of Chemistry, Cambridge, England.

Sierks, M. R., & Svensson, B. (1996) *Biochemistry 35*, 1865−1871.

Sierks, M. R., Ford, C., Reilly, P. J., & Svensson, B. (1989) *Protein Eng. 2*, 621−625.

Sierks, M. R., Ford, C., Reilly, P. J., & Svensson, B. (1990) *Protein Eng. 3*, 193−198.

Suetsugu, N., Hiromi, K., & Ono, S. (1971) *J. Biochem. (Tokyo) 69*, 421−424.

Tanaka, A., Ohnishi, M., & Hiromi, K. (1982) *Biochemistry 21*, 107−113.

BI961355R